THE JOURNAL OF PHYSICAL CHEMISTRY A

 VOLUME 113, NUMBER 32, AUGUST 13, 2009

Chaotic Synchronization under Unidirectional Coupling: Numerics and Experiments

J. M. Cruz,[†] M. Rivera,[†] and P. Parmananda*[,†,‡]

Facultad de Ciencias, UAEM, Avenida Universidad 1001, Colonia Chamilpa, C.P 62209, Cuernavaca, Morelos, Mexico, and Department of Physics, Indian Institute of Technology Bombay, Powai, Mumbai 400076, India

Received: April 12, 2009; Revised Manuscript Received: July 4, 2009

Synchronization for a pair of chaotic oscillators is studied both numerically and experimentally. The two oscillators are coupled unidirectionally, namely, in the master slave configuration. When the coupling strength is systematically varied, different regimes of chaotic synchronization such as no, phase, lag and complete are identified. The existence of natural lag synchronization for unidirectional coupling is by virtue of a small parameter mismatch between the master and the slave oscillators. Numerical calculations are carried out in the Rössler model whereas the experiments are performed using a pair of electrochemical oscillators.

1. Introduction

Synchronization of nonlinear dynamics has been studied exhaustively in diverse physical,[1−3] chemical,[4] physiological,[5] and ecological systems.[6] These synchronization phenomena can usually be observed via appropriate coupling of nonlinear systems. An alternate way to attain synchronization of nonlinear dynamics is to subject the uncoupled systems to a common external forcing. For the coupling scenario, there exist two different schemes, namely, bidirectional and unidirectional. Bidirectional coupling involves the situation wherein the two oscillators influence each other mutually. Since this bidirectional coupling is believed to be generic in a majority of natural processes, it has generated utmost interest in the scientific community. However, it is easy to motivate studying the synchronization phenomena under unidirectional coupling as there may exist numerous nonlinear processes that function within the premises of master slave configuration. The scenario for common forcing includes two uncoupled nonlinear systems subjected to a common deterministic or stochastic forcing. It is realized that while the two uncoupled nonlinear systems manifest generalized synchronization with respect to the superimposed forcing, they exhibit complete synchronization between themselves.

The synchronization phenomena persist if one chooses to work with chaotic dynamics, a special class of nonlinear behavior. Chaotic synchronization seems counterintuitive as the sensitive dependence to the initial conditions, leading to divergence of the nearby trajectories, is the signature for chaotic dynamics. This seems to be at odds with the convergence of dynamical behavior, a requirement for attainment of synchronization among coupled systems. However, the emergence of chaotic synchronization[7−10] has been verified both theoretically and experimentally in a plethora of natural processes. This concept of chaotic synchronization has attracted the attention of numerous researchers over the last 15 years and at present is being keenly investigated in the context of spatially extended systems in general and for a network of oscillators in particular. Books[11−13] and review articles[5,14] written by scientists from different areas provide testimony to the popularity and the multidisciplinary nature of this field.

In the present work, we report numerical and experimental results involving the synchronization of nonidentical (parameter mismatch) chaotic oscillators subjected to a unidirectional coupling. The main motivation for the present work was to find the entire synchronization sequence for unidirectional coupling analogous to the one already reported for the bidirectional coupling.[15−17] Systematically varying the coupling constant enabled us to identify the possible domains of the synchronization, including the first detection of natural lag synchronization for a pair of nonidentical chaotic oscillators under unidirectional coupling in a real system.[18] Lag synchronization corresponds to a state for which the amplitudes of the two oscillators are nearly identical but there exists a constant time lag between the two dynamics. Our simulations and experiments provide evidence, under unidirectional coupling, for the entire transition sequence involving transformations from a state of no synchronization → phase synchronization → lag synchronization → complete synchronization. Moreover, we present experimental results involving the induction of lag synchronization using the technique of introducing a time delay in the coupling term. Contrary to its natural lag counterpart, wherein the lag observed between the two chaotic time series depends on the system parameters, the lag provoked here is uniquely determined by the time delay introduced in the coupling term. Therefore, it is relatively easy to control/alter the lag time between the two chaotic time series.

* Corresponding author.
[†] UAEM.
[‡] Indian Institute of Technology Bombay.

10.1021/jp903365f CCC: $40.75
Published on Web 07/17/2009

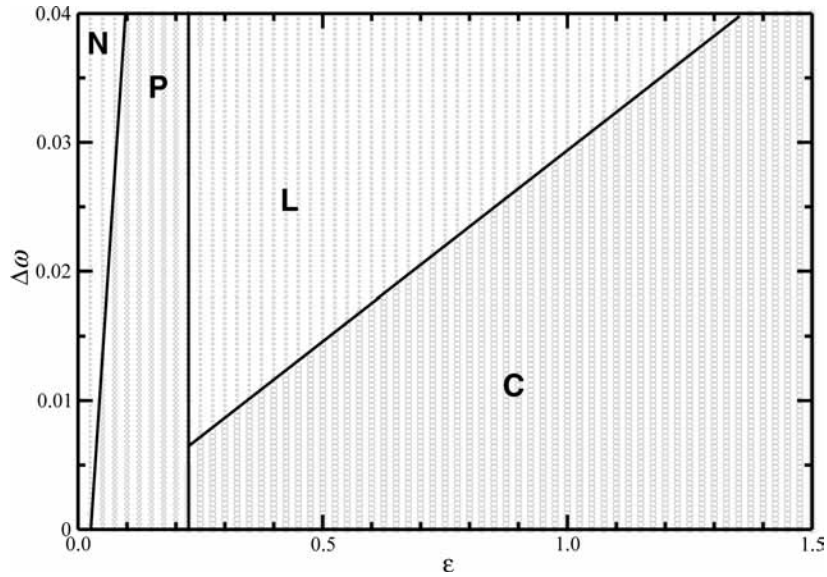

Figure 1. Numerical results, using the Rössler model, showing the different regimes of synchronization as a function of the parameter mismatch ($\Delta\omega = \omega_m - \omega_s$) and the coupling constant (ε). The labels N, P, L, C correspond to the no, phase, lag and complete synchronization domains. The model parameters are $a = 0.165$, $f = 0.2$, $c = 10.0$ and $\omega_m = 0.95$.

2. Numerical Results

To reveal the entire synchronization sequence numerically, two chaotic Rössler attractors[19] were coupled unidirectionally as shown in eqs 1−6.

$$\dot{x}_m = -\omega_m y_m - z_m \tag{1}$$

$$\dot{y}_m = \omega_m x_m + a y_m \tag{2}$$

$$\dot{z}_m = f + z_m(x_m - c) \tag{3}$$

$$\dot{x}_s = -\omega_s y_s - z_s + \varepsilon(x_m - x_s) \tag{4}$$

$$\dot{y}_s = \omega_s x_s + a y_s \tag{5}$$

$$\dot{z}_s = f + z_s(x_s - c) \tag{6}$$

The subscripts m and s correspond to the master and slave oscillators respectively. The coupling term $\varepsilon(x_m - x_s)$ is introduced in one of the evolution equations (eq 4) for the slave oscillator, and the parameter mismatch $\Delta\omega$ is determined by $(\omega_m - \omega_s)$.

Figure 1 shows the numerically generated bifurcation diagram in the $\Delta\omega$ vs ε plane revealing the location and extent of the different domains of synchronization observed. The labels N, P, L and C correspond to the no, phase, lag and complete synchronization respectively. The model parameters are presented in the corresponding figure caption. The similarity function (discussed later) calculations were used to classify the different regions of synchronization provoked.

Subsequently, keeping the parameter mismatch constant ($\Delta\omega = 0.038$), the coupling constant ε was monotonically augmented. Figure 2 shows the simulation results for the coupled chaotic Rössler oscillators. For zero coupling, the two chaotic attractors oscillate independently. Figure 2a depicts the chaotic evolution of the x_m (solid line) and x_s (dotted line) variables for the model systems. The absence of any mutual correlation between the two time series becomes more evident if one generates the x_m vs x_s plot shown in Figure 2b. The resultant attractor of Figure 2b is structureless, indicating that the dynamics are located in the domain of no synchronization. As the coupling constant ε is increased, the coupled dynamics exhibit phase synchronization. This phase synchronization effect, illustrated in the time series of Figure 2c, is characterized by the absence of correlation in the amplitude domain while in the frequency domain phase-locking is observed. The x_m vs x_s attractor for the coupled system is presented in Figure 2d. It reveals a closed curve, typical for phase synchronized dynamics. Incrementing the coupling strength further reveals the inception of lag synchronization of chaotic behavior for the coupled system. This natural lag behavior is known to be generic for bidirectionally coupled systems[15−17] with a small parameter mismatch. However, the existence of natural lag synchronization for unidirectional coupling has not yet been reported. Figure 2e shows the time series of x_m and x_s exhibiting unidirectional lag synchronization. To reiterate, lag synchronization is defined as a synchronous regime for which the states of the two oscillators are nearly identical but there exists a constant time lag between the two dynamics.

This constant time lag τ observed is an intrinsic property of the coupled oscillators. The $x_m(t - \tau)$ vs $x_s(t)$ plot, depicted in Figure 2f, reveals that the resultant attractor falls along the line of identity confirming the induction of lag synchronization. Finally, for large amplitudes of the coupling constant (ε) the chaotic dynamics, a small parameter mismatch notwithstanding, enter the regime of complete synchronization. This is evident from the superimposed time series of Figure 2g. Also, the x_m vs x_s attractor collapses on the identity line as shown in Figure 2h.

To quantify the numerical observations involving the different domains of synchronization, a similarity function[15,20] between the

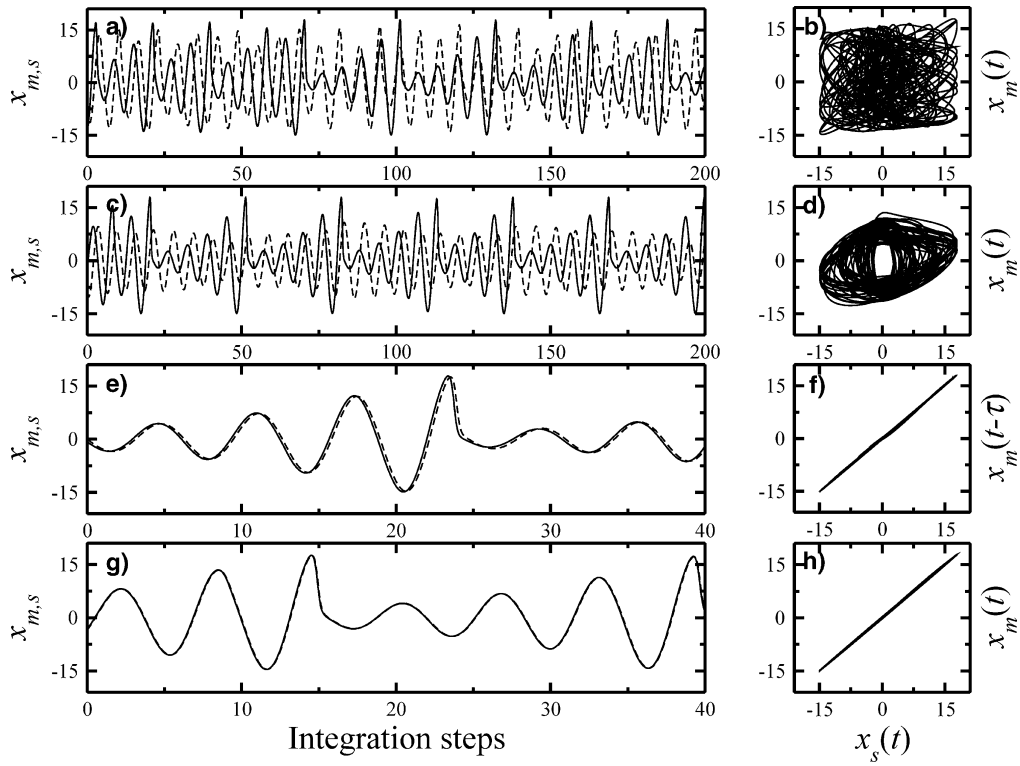

Figure 2. The different synchronization phenomena recorded as (ε) was increased monotonically. A parameter mismatch ($\Delta\omega = 0.038$), where $\omega_m = 0.95$, was introduced. The other model parameters are $a = 0.165$, $f = 0.2$, $c = 10.0$. (a) The two superimposed chaotic time series of (x_m,x_s) for $\varepsilon = 0.05$. (b) The $x_m(t)$ vs $x_s(t)$ plot for the time series of (a). For this coupling strength the dynamics were located in the domain of no synchronization. (c) The two superimposed chaotic time series of (x_m,x_s) for $\varepsilon = 0.15$. (d) The $x_m(t)$ vs $x_s(t)$ plot for the time series of (c). For this coupling strength the dynamics were located in the domain of phase synchronization. (e) The two superimposed chaotic time series of (x_m,x_s) for $\varepsilon = 0.47$. (f) The $x_m(t - \tau)$ vs $x_s(t)$ plot for the time series of (e). For this coupling strength the dynamics were located in the domain of lag synchronization. (g) The two superimposed chaotic time series of (x_m,x_s) for $\varepsilon = 1.5$. (h) The $x_m(t)$ vs $x_s(t)$ plot for the time series of (g). For this coupling strength the dynamics were located in the domain of complete synchronization.

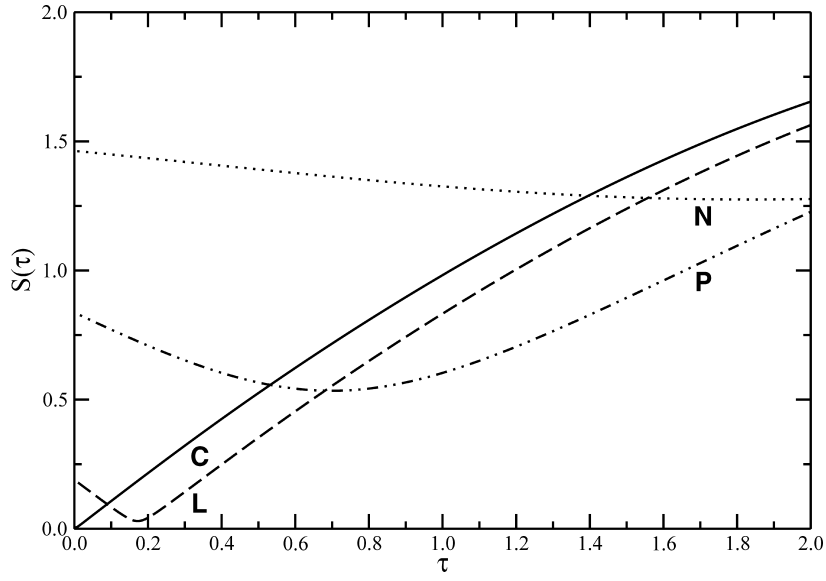

Figure 3. Similarity functions $S(\tau)$ calculated using the numerical time series presented in Figure 2. The curves labeled N, P, L, C correspond to the domains of no, phase, lag and complete synchronization respectively.

chaotic time series for the two coupled oscillators was calculated. Similarity function computes a time averaged difference between the two time series (x_m,x_s) taken with a time shift τ and is defined as

$$S^2(\tau) = \frac{\langle [x_m(t-\tau) - x_s(t)]^2 \rangle}{[\langle x_m^2(t) \rangle \langle x_s^2(t) \rangle]^{1/2}}$$

Figure 3 shows the similarity functions calculated using the numerical time series of x_m and x_s obtained for different amplitudes of the coupling constant.

The curve labeled N corresponds to simulations where the coupling constant is zero and therefore the dynamical behavior is located in the domain of no synchronization. The similarity function $S(\tau)$ for this case is practically independent

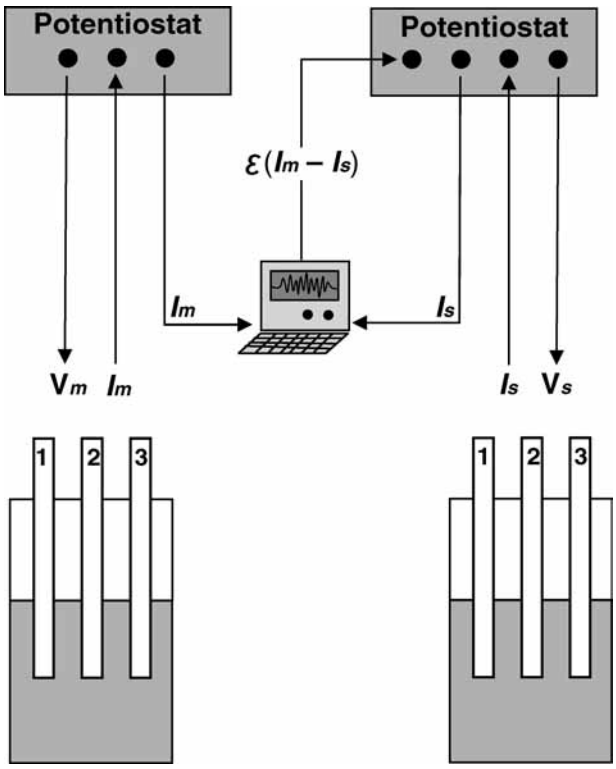

Figure 4. The schematic of the experimental setup constructed to study chaotic synchronization under unidirectional coupling. It involves two electrochemical cells with the three electrodes (labeled 1 (reference), 2 (anode), 3 (cathode)) connected via a computer in which all the relevant computations are carried out. The anodic voltage of the master cell V_m remains constant while the anodic voltage of the slave cell is continuously varied as $V_s = V_{s0} + \varepsilon(I_m - I_s)$.

of τ[15] and has an average value of $\approx\sqrt{2}$. Upon increasing the coupling constant, phase synchronization, depicted by the curve labeled P, emerges. The minimum in this curve indicates the existence of a characteristic time shift between the two chaotic time series. The appearance of lag synchronization, at higher coupling constants, is illustrated by the similarity curve labeled L. For this scenario, $S(\tau) \rightarrow 0$ for an appropriate lag time. This appropriate lag time coincides with the delay (τ) observed between the two chaotic time series of x_m and x_s shown in Figure 2e. The similarity function labeled C reveals a monotonically increasing line ($S(\tau) \rightarrow 0$ for $\tau = 0$), a behavior typical for oscillators located in the domain of complete synchronization.

3. Experimental Results

Synchronization experiments under unidirectional coupling were carried out in an electrochemical cell consisting of three electrodes, namely, anode, cathode and the reference, immersed in an electrolyte solution. The anodes were made of iron (Aldrich 99.98% purity) disks with a diameter of 6.3 mm shrouded by epoxy to ensure that the dissolution was restricted to the surface of the anode in contact with the electrolyte solution. The cathode was a graphite bar with a diameter of 6.3 mm, and the reference was the standard saturated calomel electrode (SCE). The electrolyte solution used was a mixture of 1.0 M sulfuric acid, 0.4 M potassium sulfate and 53.66 mM of potassium chloride. A volume of 250 mL was maintained in the cell.[17] The temperature of the cell was controlled to be around 300 K. The experiments were carried out potentiostatically wherein the anodic potential (V) between the anode and the reference is maintained constant. The anodic current (I) between the anode and the cathode is the system observable. The system parameter (V) is appropriately tuned such that the dynamical behavior of anodic current (I) is rendered chaotic. In contrast to our earlier work,[17] the present experimental configuration involved anodes facing downward. Moreover, the operating conditions such as volume and temperature are different. Due to these differences in the two experimental configurations the potential window for which chaotic dynamics are observed is shifted. The diagnostic tools used to characterize the anodic current time series (results no presented) were the power spectra, return maps and finally the reconstruction, using embedding, of the underlying chaotic attractor.

The biggest challenge was to configure the existing electrochemical cell to enable unidirectional coupling. This was eventually achieved by setting up a pair of bipotentiostats (PINE Model AFRDE5), each one connected to an independent electrochemical cell, used to control the two anodic potentials (V_m,V_s) individually and measure the two anodic currents (I_m,I_s) simultaneously.

Figure 4 shows the schematic of the setup employed to study chaotic synchronization under unidirectional coupling. Under the master slave configuration, V_m remains constant, whereas V_s is varied continuously by the coupling term ($\varepsilon(I_m - I_s)$) that is proportional to the difference between the anodic currents of the master (I_m) and the slave (I_s) oscillators.

Experiments were carried out to identify the different domains of synchronization exhibited by a pair of nonidentical chaotic oscillators subjected to unidirectional coupling. Apart from the inevitable inherent differences between the two electrochemical cells, a small parameter mismatch (different anodic voltages) was intentionally introduced between the two anodes. However, it was ensured that the underlying dynamics remain chaotic. Figure 5 shows the experimental results divulging the different domains of synchronization under unidirectional coupling. The anodic current time series (I_m (solid line), I_s (dotted line)) for the domains of no, phase, lag and complete synchronization are presented in the left panels whereas the resultant attractors are shown in the right panels. Analogous to the numerical results presented in the previous section, a similarity function[15,20,22] between the chaotic time series for the two coupled oscillators was calculated to quantify the experimental observations. Figure 6 shows the similarity functions computed using the anodic current time series for different coupling strengths. It clearly shows the emergence of different domains (N, P, L, C) of chaotic synchronization in the experiments. However, in contrast to the simulation results, $S(\tau)$ for experiments fails to reach zero for the lag and complete synchronization. This could be attributed to significant levels of internal noise in conjunction with a drift in the experimental dynamics.

Finally, we were also able to induce lag synchronization by introducing an intentional delay in the coupling term. Using a coupling of the form ($I_m(t - \tau) - I_s(t)$) ensures that the time series (I_s) for the slave oscillator is delayed by τ in comparison to the anodic current time series (I_m) of the master oscillator.[23] Figure 7 shows two such time series for different values of the time delay used in the coupling term.

Contrary to the natural lag, the phase shift between the two oscillators for this scenario is uniquely determined by the delay introduced in the coupling term.

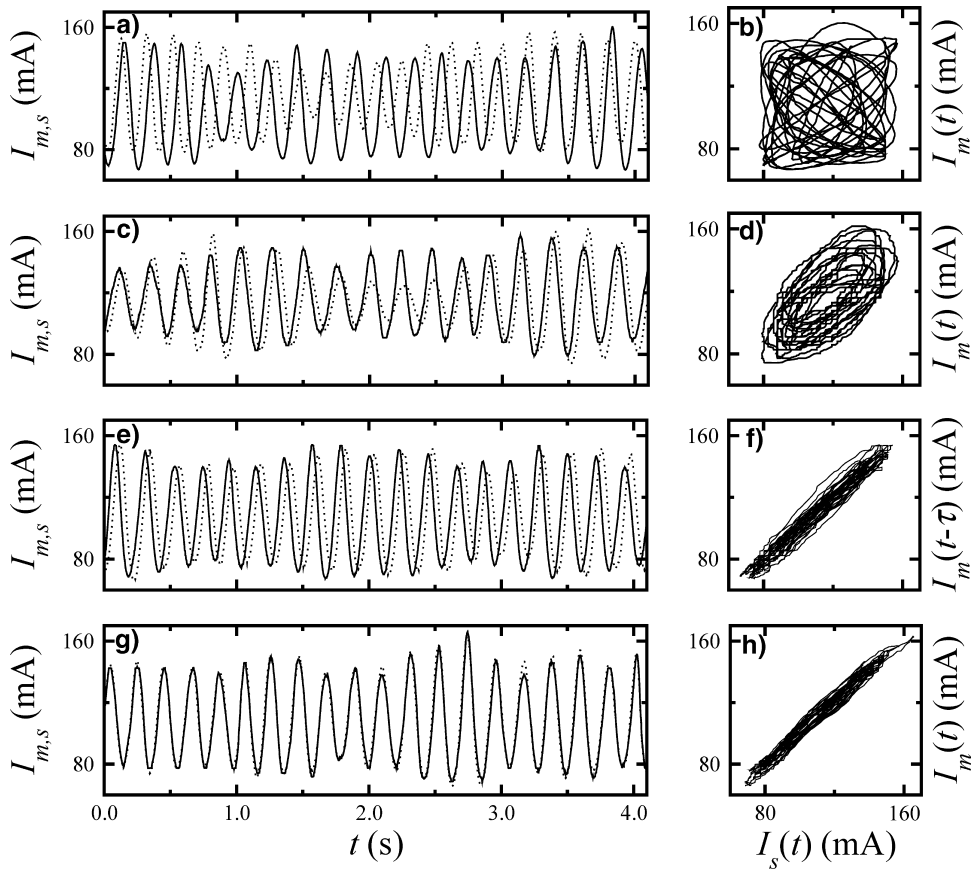

Figure 5. The different synchronization phenomena recorded as the coupling constant ε was augmented monotonically. A small parameter mismatch was introduced intentionally by choosing the two anodic voltages to be 1315 mV (V_m) and 1300 mV (V_{s0}) respectively. (a) The two superimposed chaotic time series of the anodic currents ($I_m(t)$,$I_s(t)$) where the coupling constant was chosen to be 0 mV/mA. (b) The $I_m(t)$ vs $I_s(t)$ plot for the time series of (a). For this coupling strength the dynamics were located in the domain of no synchronization. (c) The two superimposed chaotic time series of the anodic currents ($I_m(t)$,$I_s(t)$) where the coupling constant was chosen to be 0.012 mV/mA. (d) The $I_m(t)$ vs $I_s(t)$ plot for the time series of (c). For this coupling strength the dynamics were located in the domain of phase synchronization. (e) The two superimposed chaotic time series of the anodic currents ($I_m(t)$,$I_s(t)$) where the coupling constant was chosen to be 0.025 mV/mA. (f) The $I_m(t-\tau)$ vs $I_s(t)$ plot for the time series of (e). For this coupling strength the dynamics were located in the domain of lag synchronization. (g) The two superimposed chaotic time series of the anodic currents ($I_m(t)$,$I_s(t)$) where the coupling constant was chosen to be 0.12 mV/mA. (h) The $I_m(t)$ vs $I_s(t)$ plot for the time series of (g). For this coupling strength the dynamics were located in the domain of complete synchronization.

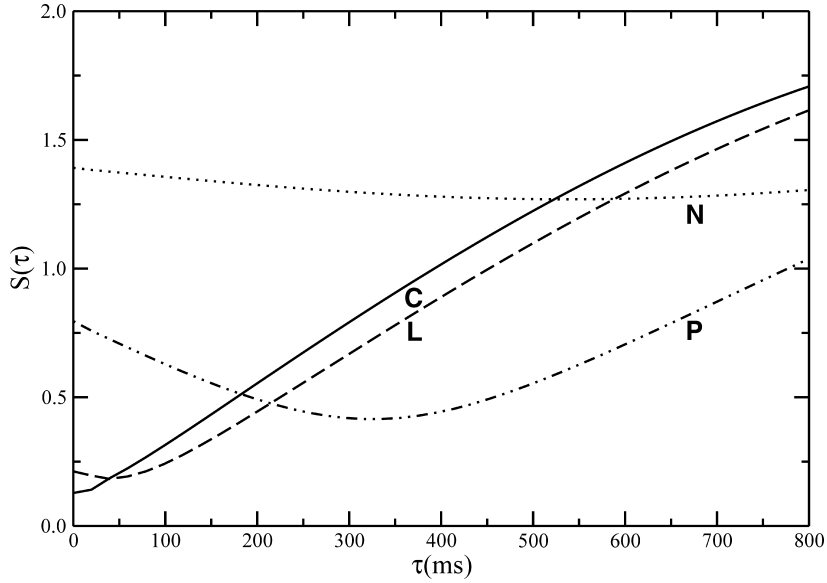

Figure 6. Similarity functions $S(\tau)$ calculated using the experimental time series of anodic currents presented in Figure 5. The curves labeled N, P, L, C correspond to the domains of no, phase, lag and complete synchronization respectively.

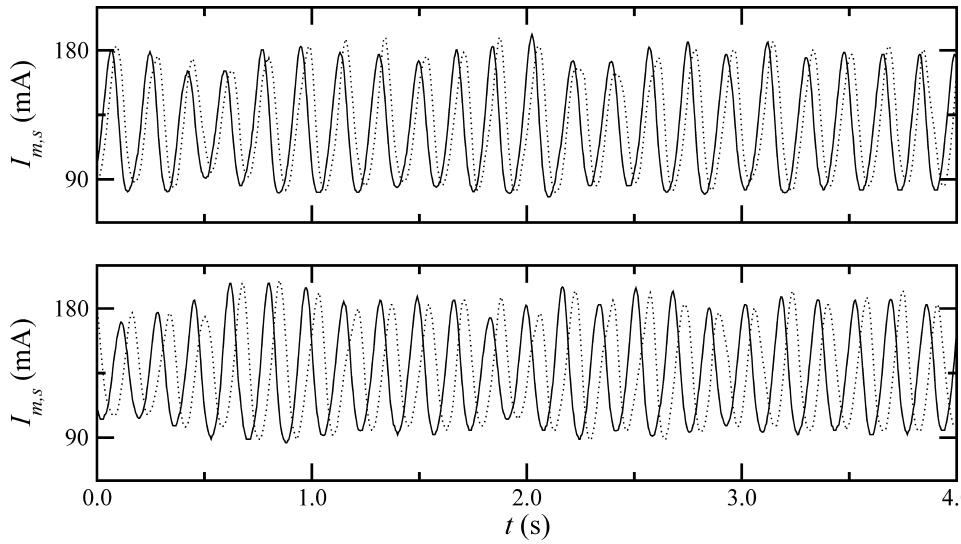

Figure 7. Artificially induced lag synchronization using an intentional delay in the coupling term. The anodic voltages were chosen to be 1315 mV (V_m) and 1300 mV (V_{s0}) respectively. The coupling constant was chosen to be 0.15 mV/mA. The upper trace corresponds to a delay of 30 ms, whereas the lower trace corresponds to a delay of 60 ms employed in the coupling term.

4. Conclusions

In conclusion, our results provide evidence of the entire transition route from the domain of no synchronization up until the region of complete synchronization for a pair of unidirectionally coupled nonidentical chaotic oscillators. The reason we chose the Rössler system for numerics was that an earlier work[15] had reported an analogous transition sequence in the Rössler model under bidirectional coupling. This included the elusive lag synchronization. So it was natural for us to take the same model and look for the corresponding sequence under unidirectional coupling. Our numerical results in conjunction with previous works[15−17] indicate that lag synchronization is independent of the nature of the underlying coupling. Furthermore, our results indicate that a necessary condition for the emergence of the lag synchronization is the parameter mismatch that generates a frequency difference between the coupled chaotic oscillators.

Moreover, the entire transition sequence found numerically could be reproduced in experiments involving coupled electrochemical cells. This included the detection of the hard to find lag synchronization. Also we were able to observe lag synchronization by suitable usage of delay in the coupling term. Using this method one can control the lag time between the master and the slave oscillator by appropriately tuning the delay introduced in the coupling term. The experimental results were obtained despite the presence of significant levels of intrinsic noise and system drift. This gives credence to the notion that the different manifestations of the synchronization phenomena under unidirectional coupling are generic in nature and therefore would persist in other real systems.

Acknowledgment. The authors acknowledge financial support from CONACyT, México.

References and Notes

(1) Thornburg, K. S., Jr.; Möller, M.; Roy, R.; Carr, T. W.; Li, R. D.; Erneux, T. *Phys. Rev. E* **1997**, *55*, 3865.
(2) Ashwin, P.; Terry, J. R.; Thornburng, K. S., Jr.; Roy, R. *Phys. Rev. E* **1998**, *6*, 7186.
(3) Masoller, C.; L. D.; de S. Cavalcante, H.; Rios Leite, J. R. *Phys. Rev. E* **2001**, *64*, 037202.
(4) Kiss, I. Z.; Gaspard, V.; Hudson, J. L. *J. Phys. Chem. B* **2000**, *104*, 7554.
(5) Glass, L. *Nature* **2001**, *410*, 277.
(6) Harrison, M. A.; Lai, Y.-Ch.; Holt, R. D. *Phys. Rev. E* **2001**, *63*, 051905.
(7) Yamada, T.; Fujisaka, H. *Prog. Theor. Phys.* **1983**, *70*, 1240.
(8) Yamada, T.; Fujisaka, H. *Prog. Theor. Phys.* **1984**, *72*, 885.
(9) Afraimovich, V. S.; Verichev, N. N.; Rabinovich, M. I. *InV. VUZ Radiofiz RPQAEC* **1986**, *29*, 795.
(10) Pecora, L. M.; Carroll, T. L. *Phys. Rev. Lett.* **1990**, *64*, 821.
(11) Pikovsky, A.; Rosenblum, M.; Kurths, J. Synchronization A Universal Concept in Nonlinear Sciences; Cambridge University Press: 2001.
(12) Strogatz, S. Sync: The Emerging Science of Spontaneous Order; Hyperion: New York, 2003.
(13) Mosekilde, E.; Maistrenko, Y.; Postnov, D. Chaotic Synchronization Applications to living Systems; World Scientific: Hackensack, NJ, 2002.
(14) Boccaletti, S.; Kurths, J.; Osipov, G.; Valladares, D. L.; Zhou, C. S. *Phys. Rep.* **2002**, *366*, 1–101.
(15) Rosenblum, M. G.; Pikovsky, A. S.; Kurths, J. *Phys. Rev. Lett.* **1997**, *78*, 4193.
(16) Rivera, M.; Martinez-Mekler, G.; Parmananda, P. *CHAOS* **2006**, *16*, 037105.
(17) Cruz, J. M.; Rivera, M.; Parmananda, P. *Phys. Rev. E* **2007**, *75*, 035201.
(18) Roy, P. K.; Chakraborty, S.; Dana, S. K. *CHAOS* **2003**, *13*, 342.
(19) Rössler, O. E. *Phys. Lett. A* **1976**, *57*, 397.
(20) Boccaletti, S.; Valladares, D. L. *Phys. Rev. E.* **2000**, *62*, 7497.
(21) Boccaletti, S.; Allaria, E.; Meucci, R.; Arecchi, F. T. *Phys. Rev. Lett.* **2002**, *89*, 194101.
(22) Sosnovtseva, O. V.; Balanov, A. G.; Vadivasova, T. E.; Astakhov, V. V.; Mosekilde, E. *Phys. Rev. E* **1999**, *60*, 6560.
(23) Shahverdiev, E. M.; Sivaprakasam, S.; Shore, K. A. *Phys. Lett. A* **2002**, *292*, 320.

JP903365F